Enhanced betatron radiation by steering a laser-driven plasma wakefield with a tilted shock front

Changhai Yu,[1] Jiansheng Liu,[1,2,a)] Wentao Wang,[1] Wentao Li,[1,3] Rong Qi,[1] Zhijun Zhang,[1] Zhiyong Qin,[1,4] Jiaqi Liu,[1,4] Ming Fang,[1,4] Ke Feng,[1,4] Ying Wu,[1,4] Lintong Ke,[1,4] Yu Chen,[1,4] Cheng Wang,[1] Yi Xu,[1] Yuxin Leng,[1] Changquan Xia,[5] Ruxin Li,[1,4,6,b)] and Zhizhan Xu[1,4,6,c)]
[1]*State Key Laboratory of High Field Laser Physics, Shanghai Institute of Optics and Fine Mechanics, Chinese Academy of Sciences, Shanghai 201800, China*
[2]*IFSA Collaborative Innovation Center, Shanghai Jiao Tong University, Shanghai 200240, China*
[3]*Department of Physics, SUPA and University of Strathclyde, Glasgow G4 0NG, United Kingdom*
[4]*University of Chinese Academy of Sciences, Beijing 100049, People's Republic of China*
[5]*College of Physical Science and Technology, Yangzhou University, Jiangsu 225001, China*
[6]*School of Physical Science and Technology, ShanghaiTech University, Shanghai 20031, China*

(Received 14 December 2017; accepted 14 March 2018; published online 27 March 2018)

We have experimentally realized a scheme to enhance betatron radiation by manipulating transverse oscillation of electrons in a laser-driven plasma wakefield with a tilted shock front (TSF). Very brilliant betatron x-rays have been produced with significant enhancement both in photon yield and peak energy but almost maintain the *e*-beam energy spread and charge. Particle-in-cell simulations indicate that the accelerated electron beam (*e* beam) can acquire a very large transverse oscillation amplitude with an increase in more than 10-fold, after being steered into the deflected wakefield due to the refraction of the driving laser at the TSF. Spectral broadening of betatron radiation can be suppressed owing to the small variation in the peak energy of the low-energy-spread *e* beam in a plasma wiggler regime. It is demonstrated that the *e*-beam generation, refracting, and wiggling can act as a whole to realize the concurrence of monoenergetic *e* beams and bright x-rays in a compact laser-wakefield accelerator. https://doi.org/10.1063/1.5019406

X-ray synchrotron radiation sources have become immensely useful tools for basic science and broad applications in biology and materials science.[1] State-of-the-art synchrotrons and free-electron lasers[2,3] based on a radiofrequency accelerator can now produce x-ray sources with unprecedented photon flux and brilliance but have hitherto been limited to huge facilities which are costly and only accessible to limited users. Over the past decade, a more compact accelerator based on the concept of laser-driven wakefield acceleration[4] has achieved significant progress in generating GeV-class electron beams (*e* beams),[5–11] which holds the great potential of becoming a better candidate to produce compact femtosecond x- and γ-ray sources.[12] In such a laser wakefield accelerator (LWFA), electrons trapped by the wakefield would witness an ultrahigh acceleration field of 100 GV/m and simultaneously experience the transverse focusing field of the wake and emit bright high-energy x-rays through the betatron radiation mechanism.[13–15]

The properties of betatron radiation are normally characterized by the strength parameter[14–16] $K = \gamma\omega_\beta r_\beta/c \approx 1.33 \times 10^{-10}\gamma^{1/2}n_e^{1/2}[\mathrm{cm}^{-3}]\cdot r_\beta[\mu\mathrm{m}]$, where r_β is the amplitude of betatron oscillation, γ is the relativistic factor of the electron, n_e is the plasma density, and ω_p and $\omega_\beta = \omega_p/(2\gamma)^{1/2}$ are the plasma and betatron frequencies, respectively. The betatron radiation spectrum is peaked at the fundamental frequency in the undulator regime for $K \leq 1$. However, in the wiggler regime for $K \gg 1$, it is broadened consisting of merged harmonics characterized by the critical frequency $\hbar\omega_c \approx 5.24 \times 10^{-24}\gamma^2 n_e[\mathrm{cm}^{-3}]r_\beta[\mu\mathrm{m}]$. The average number of photons emitted by the *e* beam in the plasma wiggler is given by $\langle\bar{N}_X\rangle \simeq (2\pi/9)(e^2/\hbar c)N_0N_eK \simeq 5.6\times10^{-3}N_0N_eK$, where N_0 is the number of betatron oscillations executed by the *e* beam and N_e is the number of wiggling electrons.[17] Therefore, an effective way to increase the photon energy and yield of betatron radiation is to increase the oscillation amplitude r_β in addition to the increasing *e*-beam charge and energy. However, in order to obtain a high-quality high-energy *e* beam, electron injection and acceleration should be carefully manipulated via a well-performed LWFA, where a large oscillation amplitude r_β has to be avoided. Some ideas of manipulating r_β to enhance betatron radiation have been demonstrated;[18–22] however, the produced x-rays had continuum spectra because the controllability was at the cost of sacrificing the *e*-beam quality. Recently, an idea of a helical plasma undulator has been proposed to produce controllable synchrotron-like radiation by inducing centroid oscillations of the laser pulse[23,24] in a plasma channel. Furthermore, some methods have also been proposed to obtain bright betatron x-rays by applying an external ultra-intense magnetic field[25,26] in the wakefield but have not been demonstrated experimentally so far.

In this letter, we have experimentally realized a scheme to enhance the betatron radiation via separating electron injection and acceleration from manipulation of the *e*-beam transverse oscillation in the wakefield. By producing a tilted

a)E-mail: michaeljs_liu@siom.ac.cn
b)E-mail: ruxinli@mail.shcnc.ac.cn
c)E-mail: zzxu@mail.shcnc.ac.cn

shock front (TSF) somewhere in the acceleration stage, the driving laser pulse can be deflected owing to the refraction, but the accelerated monoenergetic e beam can almost keep its initial propagation axis and obtain an increased transverse momentum instantly due to the axis misalignment. By this way, the high-quality e beam can be steered into the deflected laser-driven wakefield with a controllable operation both in the transverse oscillation amplitude and energy of the e beam. Very brilliant betatron x-rays in tens of keV have been generated with significant enhancement both in photon yield and peak energy.

The experiments were carried out using the femtosecond 200-TW laser system with a repetition rate of 1 Hz.[27] The 33-fs, 800-nm laser pulses with an actual on-target power of 100 TW were focused by an $f/30$ off-axis parabola, and the vacuum beam radius w_0 was measured to be 32 μm in full width at half maximum (FWHM), reaching a peak intensity of 3.6×10^{18} W/cm^2 (normalized intensity $a_0 = 1.3$). A LWFA consisting of two-segment pure helium gas jets was designed to generate high-quality e beams with a FWHM energy spread of ~3%, an integrated charge of ~50 pC, and a rms divergence of ~0.3 mrad.[28,29] The produced e beam was deflected by a 90-cm-long dipole electromagnet and measured by a Lanex phosphor screen imaged onto an intensified charge-coupled device (ICCD) camera in a single shot. A wedge-shaped face was fabricated at the top edge of the right wall of the first-segment gas cell, which was placed at the left edge of the second gas jet, to produce a tilted shock front by stopping the supersonic gas flow,[30,31] and thus, a tilted thin gas layer was formed with a higher density than the ambient one. An optical interferometer and shadowgraphy were set up to measure the plasma density distribution as shown in Fig. 1(b). It was seen that a 30-μm-thick TSF with a tilted angle of ~30° was produced. The TSF's density could be calculated roughly based on the deflection and absorption of the probe beam[32,33] through the plasma channel. The plasma densities n_{I} in front of the slab, n_{II} within the plasma slab, and n_{III} behind the slab were measured to be $(1 \pm 0.1) \times 10^{19}$, $(5 \pm 2) \times 10^{19}$, and $(6 \pm 0.5) \times 10^{18}$ cm^{-3}, respectively. This TSF was operated as a refraction slab to deflect the driving laser and thus to manipulate the e-beam transverse oscillation in the wakefield. The betatron radiation was detected by an x-ray CCD or an x-ray spectra analyzer,[28] which were placed downstream 4.7 m away from the LWFA.

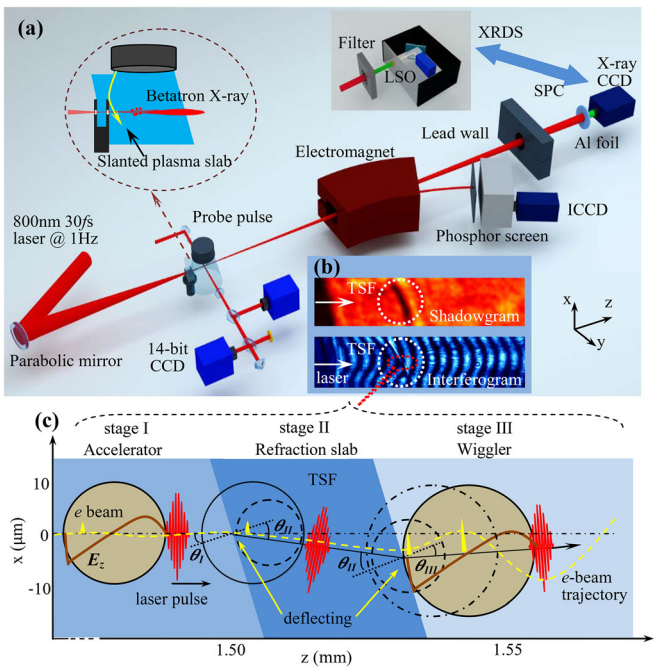

FIG. 1. (a) Experimental setup for the LWFA e-beam and betatron x-ray generation. (b) The measured TSF via an optical interferometer and a shadowgraphy. (c) A schematic diagram of using a refraction TSF to steer the e beam in a wakefield.

The physical scenario of using the TSF to steer the transverse oscillation of electrons in a laser-driven wakefield is depicted in Fig. 1(c). The refractive indices for three-segment plasmas can be calculated by $\eta = (1 - \omega_p{}^2/\gamma_\perp \omega^2)^{1/2} \approx 1 - n_e/2\gamma_\perp n_c$, where ω is the laser frequency, $\gamma_\perp$ is the relativistic factor depending on the laser intensity, and n_c is the critical density.[34,35] When the laser pulse entered the front boundary of the refraction slab, it was deflected off the incident direction with a deviation angle of $\Delta\theta_{I\to II} \approx -5.0$ mrad downward and then with $\Delta\theta_{II\to III} \approx 5.6$ mrad upward at the rear boundary, abiding by Snell's law $\eta_I \sin\theta_I = \eta_{II} \sin\theta_{II} = \eta_{III} \sin\theta_{III}$. The wakefield was deflected in the same way as the driving laser, and the accelerated e beam would thus gain an extra transverse momentum instantly due to the axis misalignment of the laser and the e beam.[24] Then, the electrons undergoing the transverse focusing of the wakefield and bending[36,37] at the boundaries would be steered from its initial propagation. Finally, the e beam generated before the TSF would obtain a much larger transverse oscillation amplitude in the plasma wiggler, where the e-beam energy would not change much if the e beam was located close to the zero-phase region of the wakefield where the accelerating field was zero.

Electron generation was investigated first by comparing the two cases when the TSF was introduced or not. As shown in Fig. 2(a), only one monoenergetic e beam with a clean background and a small divergence of ~0.2 mrad was measured. However, once the TSF was introduced, the produced e beams had a larger divergence of ~1 mrad and the peak energy varied from 259 to 351 MeV while shifting the position of the TSF from z = 1.3 to 2 mm as shown in Figs. 2(b)–2(d). The position z of the slab was defined as the distance from the entrance (z = 0) of the laser pulse into the first gas jet to the slab. Increasing z means that the length of the acceleration stage is increased. In addition to these monoenergetic e beams, some lower-energy electron tails were also observed, which might be attributed to shock-front injection.[31] The introduced TSF did not deteriorate the energy spread of e beams, and the integrated charge around the peak energy kept roughly unchanged with a similar uncertainty. However, the averaged central position shifted upward with a deflection of ~0.6 mrad while introducing the TSF, indicating that the refraction of the driving laser by the TSF affected the e-beam transverse oscillation. The uncertainty of e-beam central positions recorded at 3.6 m away from the gas jet was increased accordingly due to the larger e-beam divergence, and the e-beam pointing fluctuation was increased by almost four times in the deflection direction but still less than 1 mrad, as shown in Fig. 2(e).

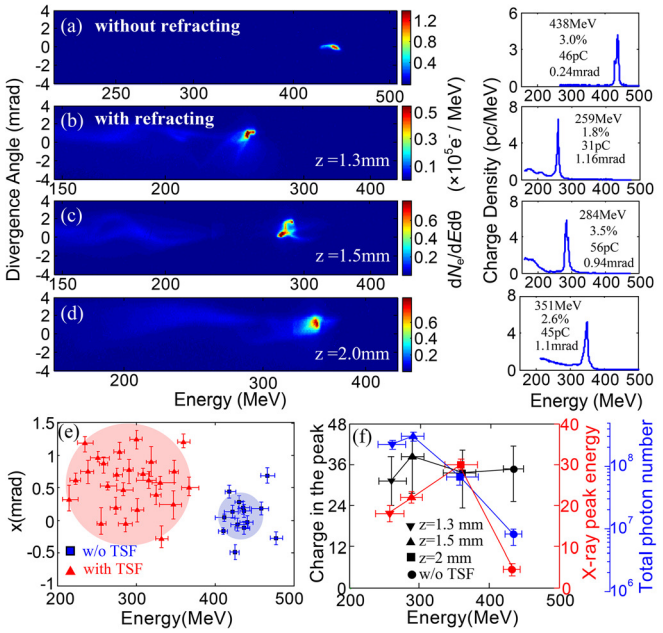

FIG. 2. (a)–(d) Single-shot typical electron spectra without and with introducing the TSF at z = 1.3, 1.5, and 2 mm, respectively. (e) Each dot represents the *e*-beam average central position over five shots without and with the TSF at different z. (f) Measured average *e*-beam charge in the peak, x-ray peak energy, and total photon number from a series of shots for each case.

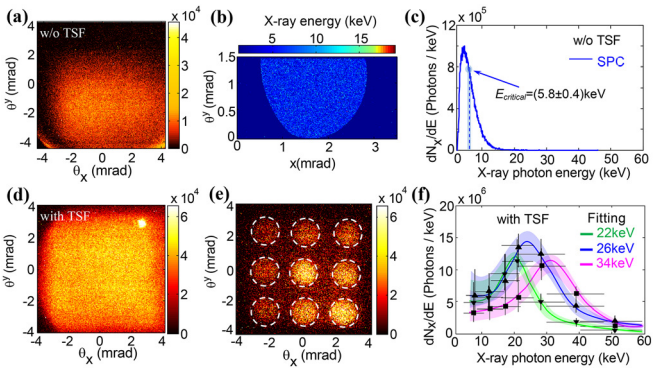

FIG. 3. (a)–(c) Typical beam patterns recorded by the XRDS, background-subtracted x-ray beam recorded on the x-ray CCD, and retrieved radiation spectra for the corresponding *e* beams in Fig. 2(a), respectively, in the case of no TSF. (d) and (e) Typical enhanced betatron x-ray beam patterns without the filter and transmitted x-ray beam profile through a 3 × 3 circle-grid filter packed with 0.1–5 mm thick attenuated sheets made of Al, Cu, and Pb materials. (f) Measured x-ray spectra with the TSF for the corresponding *e* beams in Figs. 2(b)–2(d). The shaded bands represent the spectra uncertainties.

Two techniques were employed to measure the betatron radiation spectra in a single-shot. First, in the case of no TSF when the photon yield of betatron radiation was low, a back-illuminated x-ray CCD camera operated in a single-photon-counting (SPC) mode[38,39] was used to measure the spectra below 20 keV, which could be used to measure the *e*-beam transverse emittance with a high resolution as well.[40–42] The piling events[43] could be avoided by satisfying the low photon flux requirement. Second, since the x-ray emission would be enhanced both in photon yield and photon energy after introducing the TSF, the SPC technique was not suitable any more for a much higher photon flux and higher photon energies. Then, an x-ray detection system (XRDS) based on the x-ray transmission through an array of filters[28,44,45] was designed to measure the radiation spectra. In order to avoid the influence of the driving laser on the detector, a 8-μm-thick Al film or a 300-μm-thick Be window was placed in front of the x-ray CCD camera or the Lu_2SiO_4(LSO)-crystal scintillator to block the laser.

In the case of no TSF corresponding to the *e*-beam generation at 438 MeV in Fig. 2(a), the betatron radiation patterns and retrieved radiation spectrum via the SPC are presented in Figs. 3(a)–3(c). According to the retrieved spectral profile in Fig. 3(c), the critical photon energy was estimated to be 5.8 ± 0.4 keV, indicating that the betatron oscillation amplitude r_β was less than 0.2 μm. This was slightly larger than a matched *e*-beam size of ~0.1 μm given by $\sigma_x = \sigma_\theta(\lambda_p/\pi)\sqrt{\gamma/2}$, where σ_θ is the *e*-beam divergence.[4,13,42] The undulator strength parameter was thus calculated as $K = \gamma\omega_\beta r_\beta/c \simeq 2.1$, and the number of betatron oscillation was estimated as $N_0 = L/\lambda_b \approx 5$, where L is the length of the wiggler and $\lambda_b = \sqrt{2\gamma}\lambda p$ is the betatron wavelength. The total photon yield could be predicted as $\sim 1.5 \times 10^7$. From the recorded betatron radiation pattern on the XRDS, the photon number of betatron radiation was measured to be $(1.1 \pm 0.2) \times 10^7$, in a reasonable agreement with the predicted one. The detected x-ray beam with a near-Gaussian profile had divergence angles of 2.8 and 2.2 mrad in horizontal and vertical directions, respectively, consistent with the divergence estimated by $\theta \cong K/\gamma$ (~2.5 mrad for $\gamma = 835$) around the electron velocity vector.

While introducing a TSF in the acceleration stage to enhance betatron radiation, the x-ray spectra were measured via the XRDS. Figures 3(d) and 3(e) show the recorded radiation patterns without and with inserting filters, respectively, when the TSF was introduced at z = 1.5 mm. The retrieved radiation spectra are presented in Fig. 3(f) by analyzing the signal difference transmitted through the filters.[38] It was found that the critical energy of the radiated x-ray was increased from 5.5 to 26 keV although the *e*-beam energy was decreased to 259 MeV, and the photon number which was estimated to be $(2.1 \pm 0.8) \times 10^8$ was also enhanced by more than 12-fold. Assuming that the size and duration were around 4 μm and 6 fs, the x-ray source had a peak brilliance of $\sim 10^{23}$ photons $s^{-1}\,mm^{-2}\,mrad^{-2}$ 0.1% BW. By varying the TSF position (with z increasing), the *e*-beam energy was increased from 259 to 351 MeV, and the corresponding critical photon energy of betatron radiation shifted from 22 to 34 keV in Fig. 3(f). For each of the aforementioned cases, both the statistical average x-ray photon energy and yield were increased greatly in Fig. 2(f). Besides, the enhanced betatron radiation had a larger divergence angle if compared with the case of no SPS, and the transverse coherence got worse relatively due to degradation of the transverse emittance, as shown in Figs. 3(a) and 3(d). The central position of the radiation was also shifted upward with a deviation angle of ~0.8 mrad, roughly corresponding to the deflection of the generated *e* beam.

Particle-in-cell (PIC) simulations using the Vorpal Code were carried out to get insights into the experimental results. The laser pulse parameters and plasma density profile were all chosen close to the experimental results. A linearly p-polarized Gaussian laser pulse with $\lambda_L = 800$ nm, $a_0 = 1.6$, $w_0 = 32\,\mu$m (FWHM), and $\tau_{FWHM} = 30\,fs$ was chosen, and a moving

window with a size of $75 \times 160\ \mu m^2$ was used. The grid cell size was $k_0 z = 0.209$ in the laser propagation direction, and $k_0 x = 0.393$ in the transverse direction with four macroparticles per cell. Without the TSF, one high-quality e beam can be accelerated up to a peak energy of 465 MeV, with the 3.2% FWHM energy spread, 60 μm mrad normalized emittance, and 18 pC charge, as shown in Figs. 4(c) and 4(e). The transverse oscillation amplitude is as small as 0.18 μm. However, while introducing the TSF at $z = 1.5$ mm with the tilted angle of $\theta = 26.5°$ in Fig. 4(a) and keeping other parameters the same, the deflection of the laser-driven wakefield in the vertical direction is observed in Fig. 4(b). Due to the refraction, the propagation direction of the wakefield is deflected from its initial direction in addition to an absolute offset in the vertical direction. After being steered into the deflected wakefield, the e-beam transverse radius R_b increases rapidly from 0.18 to 1.9 μm [see Figs. 4(b) and 4(d)]. The accelerated e beam is also deflected from the original laser propagation direction with a deviation angle of 0.7 mrad, in good agreement with the aforementioned measurement and analysis. While further adjusting the tilted angle of the TSF from 15° to 45°, the simulated deflection angle of the laser propagation and e beam varied from 0.29 to 0.94 mrad, as shown in Fig. 4(f), backed by the theoretical calculations obeying Snell's law. These results verified that the high-quality e beam could be steered into the deflected laser-driven wakefield to enhance the betatron radiation via introducing a TSF.

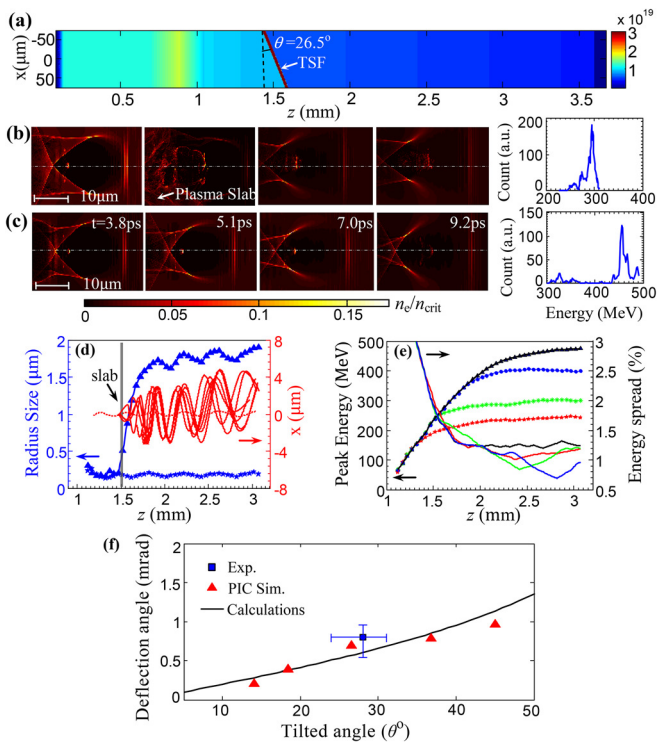

FIG. 4. (a) The plasma density distribution with the TSF. (b) and (c) Snapshots of the 2-D electron density distribution and wakefield structures for the cases with and without TSF from the PIC simulations. Both the electron spectra at $t = 9.2$ ps are plotted. (d) Transverse size for the wiggling e-beam without (blue star) and with (blue triangle) the TSF. Trajectories of accelerated electrons with (solid line) and without (dashed line) the TSF are tracked. (e) Evolution of the peak energy and rms energy spread of the e beams without (black) and with the TSF placed at $z = 1.3$ mm (red), 1.5 mm (green) and 2 mm (blue), respectively. (f) The deflection angle of the e beam due to the refraction of laser pulse, with respect to the incident direction at different tilted angles of the TSF at $z = 1.5$ mm.

Besides, the e-beam length remains the same without loss of beam charge and the energy spread can even be reduced a little, which might be attributed to energy chirp compensation due to the phase space rotation.[46,47] Some electrons might be injected into the wakefield behind the TSF owing to the shock-front injection at the transient downward density ramp,[29] but they cannot be efficiently accelerated due to the quick dephasing owing to the great density difference at the downward density ramp. However, the steered e beam slips forward quickly with respect to the wakefield to the zero-phase region, and thus, the e-beam energy varies little in the following stage. Furthermore, the FWHM energy spread of the e beams produced in our case is as small as 2.5%. These two effects and periodical oscillation in the wiggler stage are expected to reduce relatively the bandwidth of the betatron spectrum near the peak, which is supported by the simulated and theoretical spectrum calculated from the Lienard-Wiechert potentials.

In conclusion, we have experimentally realized a scheme of separating electron injection and acceleration from manipulation of the e-beam transverse oscillation. By introducing a TSF somewhere in the acceleration stage, both the transverse oscillation amplitude and energy of the e beam could be independently manipulated in the wakefield, which was supported by the PIC simulations as well. The e-beam generation, refracting, and wiggling can thus act as a whole to realize the concurrence of the monoenergetic e beam and bright x-rays in a compact LWFA. Since the radiated photon flux is proportional to the wiggler length, the radiated photon number can be increased by increasing the length of the plasma wiggler, while the spectral broadening can be suppressed further. It is anticipated that this compact monoenergetic e beam and brilliant x-ray source will provide practical applications in the ultrafast pump-probe study.

This work was supported by the National Natural Science Foundation of China (Grant Nos. 11425418, 11127901, 61521093, and 11505263), the Strategic Priority Research Program (B) (Grant No. XDB16), sponsored by Shanghai Sailing Program (Grant No. 18YF1426000), and State Key Laboratory Program of Chinese Ministry of Science and Technology.

[1]C. Bostedt, S. Boutet, D. M. Fritz, Z. R. Huang, H. J. Lee, H. T. Lemke, A. Robert, W. F. Schlotter, J. J. Turner, and G. J. Williams, Rev. Mod. Phys. **88**, 015007 (2016).
[2]D. H. Bilderback, P. Elleaume, and E. Weckert, J. Phys. B **38**, S773 (2005).
[3]M. Altarelli, High Power Laser Sci. Eng. **3**, e18 (2015).
[4]E. Esarey, C. B. Schroeder, and W. P. Leemans, Rev. Mod. Phys. **81**, 1229 (2009).
[5]S. Kneip, S. R. Nagel, S. F. Martins, S. P. Mangles, C. Bellei, O. Chekhlov, R. J. Clarke, N. Delerue, E. J. Divall, G. Doucas, K. Ertel, F. Fiuza, R. Fonseca, P. Foster, S. J. Hawkes, C. J. Hooker, K. Krushelnick, W. B. Mori, C. A. Palmer, K. T. Phuoc, P. P. Rajeev, J. Schreiber, M. J. Streeter, D. Urner, J. Vieira, L. O. Silva, and Z. Najmudin, Phys. Rev. Lett. **103**, 035002 (2009).
[6]C. E. Clayton, J. E. Ralph, F. Albert, R. A. Fonseca, S. H. Glenzer, C. Joshi, W. Lu, K. A. Marsh, S. F. Martins, W. B. Mori, A. Pak, F. S. Tsung, B. B. Pollock, J. S. Ross, L. O. Silva, and D. H. Froula, Phys. Rev. Lett. **105**, 105003 (2010).

[7]J. S. Liu, C. Q. Xia, W. T. Wang, H. Y. Lu, C. Wang, A. H. Deng, W. T. Li, H. Zhang, X. Y. Liang, Y. X. Leng, X. M. Lu, C. Wang, J. Z. Wang, K. Nakajima, R. X. Li, and Z. Z. Xu, Phys. Rev. Lett. **107**, 035001 (2011).
[8]H. T. Kim, K. H. Pae, H. J. Cha, I. J. Kim, T. J. Yu, J. H. Sung, S. K. Lee, T. M. Jeong, and J. Lee, Phys. Rev. Lett. **111**, 165002 (2013).
[9]W. T. Wang, W. T. Li, J. S. Liu, C. Wang, Q. Chen, Z. J. Zhang, R. Qi, Y. X. Leng, X. Y. Liang, Y. Q. Liu, X. M. Lu, C. Wang, R. X. Li, and Z. Z. Xu, Appl. Phys. Lett. **103**, 243501 (2013).
[10]X. Wang, R. Zgadzaj, N. Fazel, Z. Li, S. A. Yi, X. Zhang, W. Henderson, Y. Y. Chang, R. Korzekwa, H. E. Tsai, C. H. Pai, H. Quevedo, G. Dyer, E. Gaul, M. Martinez, A. C. Bernstein, T. Borger, M. Spinks, M. Donovan, V. Khudik, G. Shvets, T. Ditmire, and M. C. Downer, Nat. Commun. **4**, 1988 (2013).
[11]W. P. Leemans, A. J. Gonsalves, H. S. Mao, K. Nakamura, C. Benedetti, C. B. Schroeder, C. Toth, J. Daniels, D. E. Mittelberger, S. S. Bulanov, J. L. Vay, C. G. Geddes, and E. Esarey, Phys. Rev. Lett. **113**, 245002 (2014).
[12]S. Corde, K. Ta Phuoc, G. Lambert, R. Fitour, V. Malka, A. Rousse, A. Beck, and E. Lefebvre, Rev. Mod. Phys. **85**, 1 (2013).
[13]E. Esarey, B. A. Shadwick, P. Catravas, and W. P. Leemans, Phys. Rev. E **65**, 056505 (2002).
[14]I. Kostyukov, S. Kiselev, and A. Pukhov, Phys. Plasmas **10**, 4818 (2003).
[15]A. Rousse, K. T. Phuoc, R. Shah, A. Pukhov, E. Lefebvre, V. Malka, S. Kiselev, F. Burgy, J.-P. Rousseau, D. Umstadter, and D. Hulin, Phys. Rev. Lett. **93**, 135005 (2004).
[16]F. Albert, R. Shah, K. T. Phuoc, R. Fitour, F. Burgy, J.-P. Rousseau, A. Tafzi, D. Douillet, T. Lefrou, and A. Rousse, Phys. Rev. E **77**, 056402 (2008).
[17]S. Kiselev, A. Pukhov, and I. Kostyukov, Phys. Rev. Lett. **93**, 135004 (2004).
[18]S. Cipiccia, M. R. Islam, B. Ersfeld, R. P. Shanks, E. Brunetti, G. Vieux, X. Yang, R. C. Issac, S. M. Wiggins, G. H. Welsh, M.-P. Anania, D. Maneuski, R. Montgomery, G. Smith, M. Hoek, D. J. Hamilton, N. R. C. Lemos, D. Symes, P. P. Rajeev, V. O. Shea, J. M. Dias, and D. A. Jaroszynski, Nat. Phys. **7**, 867 (2011).
[19]A. Popp, J. Vieira, J. Osterhoff, Z. Major, R. Hörlein, M. Fuchs, R. Weingartner, T. P. Rowlands-Rees, M. Marti, R. A. Fonseca, S. F. Martins, L. O. Silva, S. M. Hooker, F. Krausz, F. Grüner, and S. Karsch, Phys. Rev. Lett. **105**, 215001 (2010).
[20]K. Ta Phuoc, E. Esarey, V. Leurent, E. Cormier-Michel, C. G. R. Geddes, C. B. Schroeder, A. Rousse, and W. P. Leemans, Phys. Plasmas **15**, 063102 (2008).
[21]L. M. Chen, W. C. Yan, D. Z. Li, Z. D. Hu, L. Zhang, W. M. Wang, N. Hafz, J. Y. Mao, K. Huang, Y. Ma, J. R. Zhao, J. L. Ma, Y. T. Li, X. Lu, Z. M. Sheng, Z. Y. Wei, J. Gao, and J. Zhang, Sci. Rep. **3**, 1912 (2013).
[22]W. Yan, L. Chen, D. Li, L. Zhang, N. A. Hafz, J. Dunn, Y. Ma, K. Huang, L. Su, M. Chen, Z. Sheng, and J. Zhang, Proc. Natl. Acad. Sci. U. S. A. **111**, 5825 (2014).
[23]S. G. Rykovanov, C. B. Schroeder, E. Esarey, C. G. R. Geddes, and W. P. Leemans, Phys. Rev. Lett. **114**, 145003 (2015).
[24]M. Chen, J. Luo, F.-Y. Li, F. Liu, Z.-M. Sheng, and J. Zhang, Light: Sci. Appl. **5**, e16015 (2016).
[25]Z. M. Zhang, B. Zhang, W. Hong, M. Y. Yu, Z. G. Deng, J. Teng, S. K. He, and Y. Q. Gu, Plasma Phys. Controlled Fusion **58**, 105009 (2016).
[26]K. Q. Pan, C. Y. Zheng, L. H. Cao, Z. J. Liu, and X. T. He, Phys. Plasmas **23**, 043115 (2016).
[27]Y. Xu, J. Lu, W. Li, F. Wu, Y. Li, C. Wang, Z. Li, X. Lu, Y. Liu, Y. Leng, R. Li, and Z. Xu, Opt. Laser Technol. **79**, 141 (2016).
[28]C. H. Yu, R. Qi, W. T. Wang, J. S. Liu, W. T. Li, C. Wang, Z. J. Zhang, J. Q. Liu, Z. Y. Qin, M. Fang, K. Feng, Y. Wu, Y. Tian, Y. Xu, F. X. Wu, Y. X. Leng, X. F. Weng, J. H. Wang, F. L. Wei, Y. C. Yi, Z. H. Song, R. X. Li, and Z. Z. Xu, Sci. Rep. **6**, 29518 (2016).
[29]W. T. Wang, W. T. Li, J. S. Liu, Z. J. Zhang, R. Qi, C. H. Yu, J. Q. Liu, M. Fang, Z. Y. Qin, C. Wang, Y. Xu, F. X. Wu, Y. X. Leng, R. X. Li, and Z. Z. Xu, Phys. Rev. Lett. **117**, 124801 (2016).
[30]K. Schmid, A. Buck, C. M. S. Sears, J. M. Mikhailova, R. Tautz, D. Herrmann, M. Geissler, F. Krausz, and L. Veisz, Phys. Rev. ST Accel. Beams **13**, 091301 (2010).
[31]A. Buck, J. Wenz, J. Xu, K. Khrennikov, K. Schmid, M. Heigoldt, J. M. Mikhailova, M. Geissler, B. Shen, F. Krausz, S. Karsch, and L. Veisz, Phys. Rev. Lett. **110**, 185006 (2013).
[32]L. B. Dasilva, T. W. Barbee, R. Cauble, P. Celliers, D. Ciarlo, S. Libby, R. A. London, D. Matthews, S. Mrowka, J. C. Moreno, D. Ress, J. E. Trebes, A. S. Wan, and F. Weber, Phys. Rev. Lett. **74**, 3991 (1995).
[33]D. Ress, L. B. Dasilva, R. A. London, J. E. Trebes, S. Mrowka, R. J. Procassini, T. W. Barbee, Jr., and D. E. Lehr, Science **265**, 514 (1994).
[34]E. Esarey, P. Sprangle, J. Krall, and A. Ting, IEEE. Trans. Plasma Sci. **24**, 252 (1996).
[35]P. Monot, T. Auguste, P. Gibbon, F. Jakober, G. Mainfray, A. Dulieu, M. Louis-Jacquet, G. Malka, and J. L. Miquel, Phys. Rev. Lett. **74**, 2953 (1995).
[36]P. Muggli, S. Lee, T. Katsouleas, R. Assmann, F. J. Decker, M. J. Hogan, R. Iverson, P. Raimondi, R. H. Siemann, D. Walz, B. Blue, C. E. Clayton, E. Dodd, R. A. Fonseca, R. Hemker, C. Joshi, K. A. Marsh, W. B. Mori, and S. Wang, Nature **411**, 43 (2001).
[37]T. Katsouleas, W. B. Mori, E. Dodd, S. Lee, R. Hemker, C. Clayton, C. Joshi, and E. Esarey, Nucl. Instrum. Methods A **455**, 161 (2000).
[38]D. B. Thorn, C. G. R. Geddes, N. H. Matlis, G. R. Plateau, E. H. Esarey, M. Battaglia, C. B. Schroeder, S. Shiraishi, T. Stöhlker, C. Tóth, and W. P. Leemans, Rev. Sci. Instrum. **81**, 10E325 (2010).
[39]S. Fourmaux, S. Corde, K. Ta Phuoc, P. M. Leguay, S. Payeur, P. Lassonde, S. Gnedyuk, G. Lebrun, C. Fourment, V. Malka, S. Sebban, A. Rousse, and J. C. Kieffer, New J. Phys. **13**, 033017 (2011).
[40]A. Curcio, M. Anania, F. Bisesto, E. Chiadroni, A. Cianchi, M. Ferrario, F. Filippi, D. Giulietti, A. Marocchino, F. Mira, M. Petrarca, V. Shpakov, and A. Zigler, Appl. Phys. Lett. **111**, 133105 (2017).
[41]A. Curcio, M. Anania, F. Bisesto, E. Chiadroni, A. Cianchi, M. Ferrario, F. Filippi, D. Giulietti, A. Marocchino, M. Petrarca, V. Shpakov, and A. Zigler, Phys. Rev. ST Accel. Beams **20**, 012801 (2017).
[42]G. R. Plateau, C. G. R. Geddes, D. B. Thorn, M. Chen, C. Benedetti, E. Esarey, A. J. Gonsalves, N. H. Matlis, K. Nakamura, C. B. Schroeder, S. Shiraishi, T. Sokollik, J. van Tilborg, C. Toth, S. Trotsenko, T. S. Kim, M. Battaglia, T. Stöhlker, and W. P. Leemans, Phys. Rev. Lett. **109**, 064802 (2012).
[43]C. Fourment, N. Arazam, C. Bonte, T. Caillaud, D. Descamps, F. Dorchies, M. Harmand, S. Hulin, S. Petit, and J. J. Santos, Rev. Sci. Instrum. **80**, 083505 (2009).
[44]K. Ta Phuoc, S. Corde, C. Thaury, V. Malka, A. Tafzi, J. P. Goddet, R. C. Shah, S. Sebban, and A. Rousse, Nat. Photonics **6**, 308 (2012).
[45]N. D. Powers, I. Ghebregziabher, G. Golovin, C. Liu, S. Chen, S. Banerjee, J. Zhang, and D. P. Umstadter, Nat. Photonics **8**, 28 (2014).
[46]F. S. Tsung, R. Narang, W. B. Mori, C. Joshi, R. A. Fonseca, and L. O. Silva, Phys. Rev. Lett. **93**, 185002 (2004).
[47]S. Y. Kalmykov, A. Beck, S. A. Yi, V. N. Khudik, M. C. Downer, E. Lefebvre, B. A. Shadwick, and D. P. Umstadter, Phys. Plasmas **18**, 056704 (2011).